Date: September 15, 2004 COST279TD(04)029
Issue: 1

Spatial Node Distribution in the Random Waypoint Mobility Model

Esa Hyytiä, Pasi Lassila, Laura Nieminen and Jorma Virtamo[1]

Networking Laboratory, Helsinki University of Technology,
P.O. Box 3000, FIN 02015 HUT, Finland

Abstract

The random waypoint model (RWP) is one of the most widely used mobility models in performance analysis of ad hoc networks. We analyze two key properties of the RWP model in a given convex area: the stationary spatial distribution for the location of the node and the mean length of a leg (line between two waypoints). A general expression is given for the spatial node distribution in the form of a one-dimensional integral, giving the density up to a normalization constant. The mean length of a leg can be obtained through the normalization constant or by an alternative expression in the form of a two-dimensional integral. Similar analytical results are also given for a modified version of RWP, where the waypoints are chosen randomly on the perimeter. Additionally, we utilize our analytical results and present several simulation methods that allow an efficient generation of samples from the spatial node distribution. The analytical results are illustrated through numerical examples.

1 Introduction

Analysis of wireless systems, either via simulation or analytical modeling, often requires that the effect of node (or user) mobility on system performance can be modelled. The construction and use of mobility models based on the actual, say, measured characteristics of mobile nodes is difficult. Thus, one often uses simple synthetic mobility models instead, which still capture the essential impact of mobility on the performance issue under study. The advantage of using synthetic models is that they can be more easily treated in analysis or implemented in simulations. In this context, also analyzing the properties of the mobility

[1]email: Esa.Hyytia@iki.fi, {Pasi.Lassila,Laura.Nieminen,Jorma.Virtamo}@hut.fi

models is necessary. For example, one important intrinsic property of any mobility model is the distribution of the node location (or shortly the node distribution), which may be far from uniform. Knowledge about this distribution can, for example, be used to study the impact of a non-uniform node distribution vs. the common assumption of uniformly located nodes (as in capacity studies, for example [1], [2]; or connectivity studies, for example [3] or [4]).

One of the most widely used synthetic mobility models is the Random Waypoint model (RWP), which was originally proposed for studying the performance of ad hoc routing protocols by Johnson and Maltz [5]. In this model, a mobile node moves along a zigzag line, where each of the straight line segments is called *a leg*. At each turning point the node chooses a new destination randomly and then moves towards the destination at a constant speed, which is drawn independently from a given speed distribution at each turning point. The node may also remain stationary for a random think time before starting its movement towards the new destination.

In this paper, we focus on particular spatial properties of the RWP model, namely the node distribution and mean length of a leg, i.e., the mean distance between two arbitrary turning points. Previous work in [6], [7], [8] and [9] contain results for some special geometries (line, circle, rectangle) but no general expression for the node distribution has been given. Moreover, the results in [7] (and restated in [8]) on the circle and rectangle geometries are only approximate, though quite accurate ones.

We derive a general analytical expression for the node distribution and the mean length of a leg in an arbitrary convex region. Direct application of the definition for the node distribution requires integration over the locations of all possible starting and ending points resulting in a four-dimensional integral. We are able to simplify the expression to a one-dimensional integral, which gives the distribution up to a normalization constant. The evaluation of the normalization constant requires integration of the density expression over the considered region. The mean length of a leg can be related to the normalization constant. On the other hand, it can be expressed as a four-dimensional integral which we reduce to a two-dimensional one. Thus, we have two alternative expressions. The results are illustrated for various geometries (unit circle, rectangle, general polygon and line).

Similar results are presented for a variant of the RWP model, named as RWPB, where the waypoints are located on the perimeter of the area. For the case of unit circle, explicit results can be obtained, whereas in [6] the same system has been analyzed using simulation.

Additionally, we address a problem frequently encountered in many simulation studies of ad hoc networks, namely the efficient generation of sample points from the RWP model. Several methods are given to generate independent samples of the RWP movement process representing a node's location at a random instant of time. The performance of the methods is assessed through some numerical examples.

The rest of the paper is organized as follows. Section 2 introduces the traditional RWP model and its variant RWPB, together with some of the notation. The RWP model is analyzed in Section 3, where analytic expressions for the node distribution and the mean

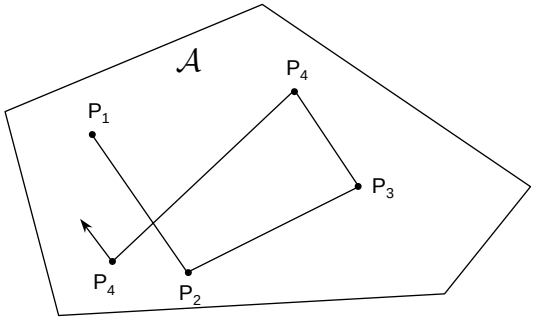

Figure 1: Zigzag movement of the RWP process.

length of a leg are derived and illustrated for several geometries. Correspondingly, the results for RWPB are given in Section 4. Efficient simulation of RWP models is discussed in Section 5 and Section 6 contains our conclusions.

2 Random Waypoint mobility model

The RWP mobility model for evaluating the performance of ad hoc routing protocols was first proposed in [5] (however, the name RWP was introduced later in [10]). Since then it has been used in numerous simulation studies.

The process representing the movement of a node within a convex area $\mathcal{A} \subset \mathbb{R}^2$ according to the RWP model can be described as follows. Initially, the node is placed at the point P_1 chosen from a uniform distribution over $\mathcal{A}$. Then a destination point (also called waypoint) P_2 is chosen from a uniform distribution over $\mathcal{A}$ and the node moves along a straight line from P_1 to P_2 with constant velocity V_1 drawn independently of the location from a distribution with pdf $f_V(v)$. Once the node reaches P_2, a new destination point, P_3, is drawn independently from a uniform distribution over $\mathcal{A}$ and velocity V_2 is drawn from $f_V(v)$ independently of the location and V_1. The node again moves at constant velocity V_2 to the point P_3, and the process repeats. This is illustrated in Figure 1. Thus, the path of a node consists of straight line segments, also called legs, defined by a sequence of independently and uniformly distributed waypoints, $\{P_i\}$, in a convex set $\mathcal{A} \subset \mathbb{R}^2$. Furthermore, on each leg (P_{i-1}, P_i) the node velocity V_i is an i.i.d. random variable having the pdf $f_V(v)$, which is also independent of the node location.

Next we introduce some notation used throughout our analysis of RWP. Let random variable $\mathbf{X}$ denote the location of a waypoint P. The waypoints are uniformly and independently distributed over $\mathcal{A}$, i.e., the probability density function (pdf) of $\mathbf{X}$ is

$$f_{\mathrm{RWP}}(\mathbf{r}) = \begin{cases} \dfrac{1}{A}, & \mathbf{r} \in \mathcal{A}, \\ 0, & \text{otherwise}, \end{cases}$$

where $A \subset \mathbb{R}^2$ denotes the area of the set $\mathcal{A}$. We denote this uniform distribution by $\mathrm{U}(\mathcal{A})$

and write $\mathbf{X} \sim \mathrm{U}(\mathcal{A})$. The random variable representing the location of the node at an arbitrary point of time is denoted by $\mathbf{R}$ and its pdf by $f(\mathbf{r})$.

Impact of velocity distribution: Originally in [5], the velocities were taken from a uniform distribution in the range $[v_{\min}, v_{\max}]$, but any distribution can be used (e.g., the beta distribution and a discrete distribution have been used in [8]). Given the pdf $f_V(v)$ from which the velocities at the waypoints are drawn, the stationary distribution of the velocity for a node moving according to the RWP model is given by $(1/v)f_V(v)$ up to a normalization constant. This is because the time spent on a leg is proportional to $1/v$, and V and $\mathbf{X}$ are independent. From this it is also obvious that for $f_V(v) = \mathrm{U}[v_{\min}, v_{\max}]$ the stationary distribution is only defined for $v_{\min} > 0$. Hence, studies letting $v_{\min} = 0$ as in [11] are not really meaningful because stationarity is never reached or, more precisely, in the stationary state all the nodes are stopped. This comment is also made in [8]. Finally, note that the stationary distribution of the location of a node and the stationary node velocity distribution are independent of each other.

RWP with think times: The RWP model also allows a node to pause for a random think time at a waypoint $\mathbf{X}$. The influence of this generalization on the node location distribution can be analyzed in a rather straight forward manner. The case where the think times are chosen independently of previous think times and also independently of the location is discussed in [8], but we can easily generalize the setting to allow the think time to depend on the location of the waypoint. Let us denote the random variable for the think time by S. It is easy to see that when think times are included in the model, the process $\mathbf{R}(t)$ basically consists of two independent modes, mobile and stagnant. The node location distribution $f^{(\mathrm{t})}(\mathbf{r})$ is given by a weighted combination of the mobile component, $f(\mathbf{r})$, and the stagnant component which is simply the distribution of the waypoint locations, $f_{\mathrm{RWP}}(\mathbf{r})$,

$$f^{(\mathrm{t})}(\mathbf{r}) = p_m f(\mathbf{r}) + p_s(\mathbf{r}) f_{\mathrm{RWP}}(\mathbf{r}),$$

where p_m and $p_s(\mathbf{r})$ represent the proportions of time the process is mobile (independent of the location) and stagnant at location $\mathbf{r}$, respectively. The probabilities p_m and $p_s(\mathbf{r})$ are given by

$$p_m = \frac{\mathrm{E}[M]}{\mathrm{E}[M] + \mathrm{E}[S]} \quad \text{and} \quad p_s(\mathbf{r}) = \frac{\mathrm{E}\left[S \,|\, \mathbf{X} = \mathbf{r}\right]}{\mathrm{E}[M] + \mathrm{E}[S]},$$

where $\mathrm{E}[S]$ is the expected length of the think time given by $\mathrm{E}[S] = \int \mathrm{E}\left[S \,|\, \mathbf{X} = \mathbf{r}\right] f_{\mathrm{RWP}}(\mathbf{r})\, d^2\mathbf{r}$ and $\mathrm{E}[M]$ is the expected duration of a transition between two waypoints given by $\mathrm{E}[M] = \int (\overline{\ell}/v) f_V(v) dv$ with $\overline{\ell}$ denoting the mean length of a leg. In the rest of this paper we assume, for simplicity, that the node does not have any think times and we focus on the derivation of $f(\mathbf{r})$ and $\overline{\ell}$.

2.1 RWP-on-the-Border

The RWPB (RWP-on-the-Border) model is a modified version of the RWP model. The basic principle is similar as in the RWP model, but each waypoint P is located on the perimeter

of the area $\mathcal{A}$, which we denote by $\mathcal{B}$. We distinguish between two different ways of selecting the P:

- The waypoints P are chosen from a uniform distribution on the perimeter of $\mathcal{A}$. For this alternative a general analytic expression is given for the distribution of the location of a node.
- After arriving at waypoint P on the perimeter the node chooses the direction of motion $\phi \in [-\pi/2, \pi/2]$ with respect to a normal vector to the perimeter at P from a given angle distribution independently of the location and previous angles, and proceeds along a straight line in that direction until the perimeter is reached. This variant is studied in detail in the case of a unit circle.

3 Analysis of the RWP model

In this section the traditional RWP model (without think times) is considered. General expressions for the node distribution and the mean length of a leg are derived first. The results are then illustrated for some simple geometries (unit circle, rectangle, general polygon).

3.1 Node distribution and mean length of a leg

Node distribution: Consider a convex area $\mathcal{A}$ and a node moving within this area at a constant speed according to the RWP from waypoint P_1 at $\mathbf{r}_1$ to waypoint P_2 at $\mathbf{r}_2$. Our aim is to derive the probability density $f(\mathbf{r})$ giving the probability per unit area of finding the node at $\mathbf{r}$.

To this end consider a small area element dA located at $\mathbf{r}$. Let P_1 and P_2 be two consecutive points on the path. Denote by ℓ the line segment or leg $\overline{P_1P_2}$. The desired probability density is

$$f(\mathbf{r}) = \frac{1}{\overline{\ell}} \frac{\mathrm{E}[\ell \cap dA]}{dA},$$

i.e., the ratio of expected length of the leg ℓ segment inside dA to the average leg length $\overline{\ell}$, or the expected proportion of time spent in dA, divided by dA (probability per unit area).

The expectation in the numerator is calculated by conditioning on the position $\mathbf{r}_1$ of the point P_1,

$$\mathrm{E}[\ell \cap dA] = \frac{1}{A} \int_{\mathcal{A}} \mathrm{E}\left[\ell \cap dA \,|\, \mathbf{r}_1\right] d^2\mathbf{r}_1.$$

The conditional expectation (expectation over all possible locations of P_2) is written as

$$\mathrm{E}\left[\ell \cap dA \,|\, \mathbf{r_1}\right] = \frac{1}{A} \int_{\mathcal{A}} |\ell(\mathbf{r_1}, \mathbf{r_2}) \cap dA| \, d^2\mathbf{r}_2,$$

where we have made it explicit that the line segment ℓ is from $\mathbf{r}_1$ to $\mathbf{r}_2$.

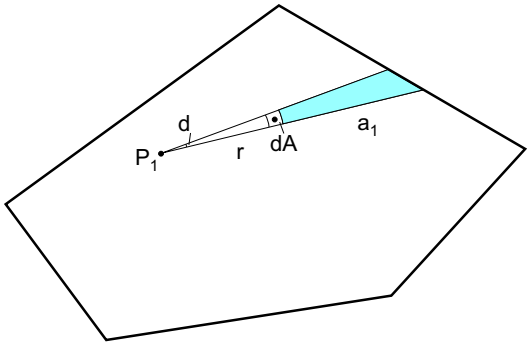

Figure 2: Illustration of the variables $P_1, d\phi, r, \Delta, dA$ and a_1.

Now refer to Figure 2, where the shape of the area dA has been chosen in a special way to facilitate the derivation. (It is easy to see that the result is the same irrespective of the shape of dA.) The intersection of $\ell(\mathbf{r_1}, \mathbf{r_2})$ and dA is Δ when $\mathbf{r}_2$ is in the shaded area and 0 otherwise. So the integral equals Δ times the shaded area and we have with the notation of the figure,

$$\mathrm{E}\,[\ell \cap dA \,|\, \mathbf{r_1}] = \frac{1}{A}\,\Delta\,\frac{1}{2}\,d\phi\,((r+a_1)^2 - r^2) = \frac{dA}{2\,A\,r}(2\,r\,a_1 + a_1^2),$$

since $dA = \Delta\, r\, d\phi$. Substitution into the original definition gives,

$$f(\mathbf{r}) = \frac{1}{\overline{\ell} A^2}\int_{\mathcal{A}} \frac{2\,r\,a_1 + a_1^2}{2\,r}\,d^2\mathbf{r}_1 = \frac{1}{\overline{\ell} A^2}\int_0^{2\pi} d\phi \int_0^{a_2} (r\,a_1 + \frac{1}{2}a_1^2)\,dr.$$

where, in the second form, polar coordinates have been used, $d^2\mathbf{r}_1 = r\,dr\,d\phi$, and a_2 denotes the distance shown in Figure 3. The radial integral can be evaluated explicitly, yielding the final result

$$f(\mathbf{r}) = \frac{1}{\overline{\ell} A^2}\int_0^{2\pi} \frac{1}{2}\,a_1 a_2 (a_1 + a_2)\,d\phi = \frac{1}{\overline{\ell} A^2}\int_0^{\pi} a_1 a_2 (a_1 + a_2)\,d\phi, \tag{1}$$

where both a_1 and a_2 are functions of $\mathbf{r}$ and ϕ, $a_1 = a_1(\mathbf{r}, \phi)$ and $a_2 = a_2(\mathbf{r}, \phi)$. The latter form follows because $a_2(\mathbf{r}, \phi) = a_1(\mathbf{r}, \phi + \pi)$, i.e., adding π to ϕ interchanges the roles of a_1 and a_2. The integration turns "the propeller" one turn around, see Figure 3. For future purposes, we denote the latter integral in (1) by $h(\mathbf{r})$,

$$h(\mathbf{r}) = \int_0^{\pi} a_1 a_2 (a_1 + a_2)\,d\phi. \tag{2}$$

Mean length of a leg: Because $f(\mathbf{r})$ is a distribution integrating to unity, we immediately obtain

$$\overline{\ell} = \frac{1}{A^2}\int_{\mathcal{A}} h(\mathbf{r})\,d^2\mathbf{r}. \tag{3}$$

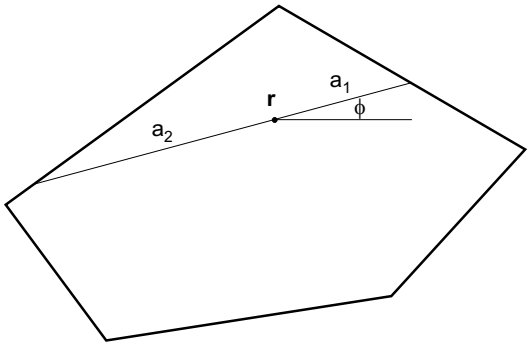

Figure 3: Illustration of the integral over $[0, 2\pi]$ in (1).

Alternatively, we can calculate $\overline{\ell}$ directly based on its definition as the average distance between two points randomly located in the area $\mathcal{A}$,

$$\overline{\ell} = \frac{1}{A^2} \int_{\mathcal{A}} d^2\mathbf{r}_1 \int_{\mathcal{A}} d^2\mathbf{r}_2 \, |\mathbf{r}_2 - \mathbf{r}_1|.$$

Instead of $\mathbf{r}_2$ we use a new variable of integration, $\mathbf{r} = \mathbf{r_2} - \mathbf{r_1}$,

$$\overline{\ell} = \frac{1}{A^2} \int d^2\mathbf{r}_1 \int d^2\mathbf{r} \; 1_{\mathbf{r}_1 \in \mathcal{A}} \, 1_{\mathbf{r}_1 + \mathbf{r} \in \mathcal{A}} \, r,$$

and define

$$B(\mathbf{r}) = \int d^2\mathbf{r}_1 \; 1_{\mathbf{r}_1 \in \mathcal{A}} \, 1_{\mathbf{r}_1 + \mathbf{r} \in \mathcal{A}} = \int d^2\mathbf{r}_1 \; 1_{\mathbf{r}_1 \in \mathcal{A} \cap (\mathcal{A} - \mathbf{r})}$$

as the area of the intersection of $\mathcal{A}$ and its copy translated by the vector $-\mathbf{r}$, yielding

$$\overline{\ell} = \frac{1}{A^2} \int d^2\mathbf{r} \; rB(\mathbf{r}) = \frac{1}{A^2} \int_0^D dr \int_0^{2\pi} d\phi \; r^2 B(r, \phi). \tag{4}$$

It obvious that $B(\mathbf{r}) = B(-\mathbf{r})$ as the area of the intersection depends only on the relative positions. The translation operation and the function $B(\mathbf{r})$ are illustrated in Figure 4. The integration in (4) is formally over the whole plane. Note, however, that $B(\mathbf{r}) = B(r, \phi)$ is zero for any translation longer than the greatest diameter D of the area $\mathcal{A}$. The new expression (4) for $\overline{\ell}$ is equivalent with (3), though this is not apparent by just looking at the expressions.

3.2 Example: unit disk

We calculate the node distribution in a unit disk with $A = \pi$. Because of the symmetry the density is a function of the distance $r = |\mathbf{r}|$ only and we write with slight abuse of notation $f(\mathbf{r}) = f(r)$. We can take any point $\mathbf{r}$ with $|\mathbf{r}| = r$; in particular we choose $\mathbf{r} = (0, r)$. Then we see from Figure 5 that

$$\begin{aligned} a_1(r, \phi) &= \sqrt{1 - r^2 \cos^2 \phi} - r \sin \phi, \\ a_2(r, \phi) &= \sqrt{1 - r^2 \cos^2 \phi} + r \sin \phi. \end{aligned}$$

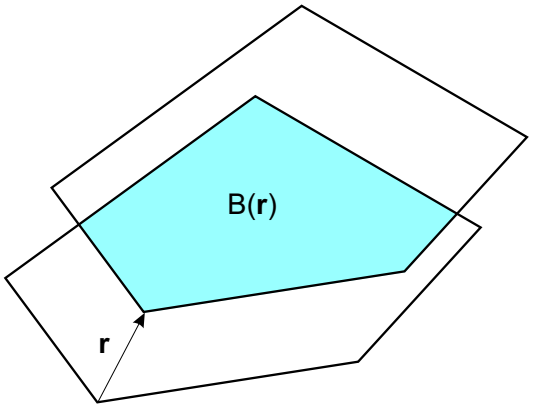

Figure 4: Illustration of the translation operation.

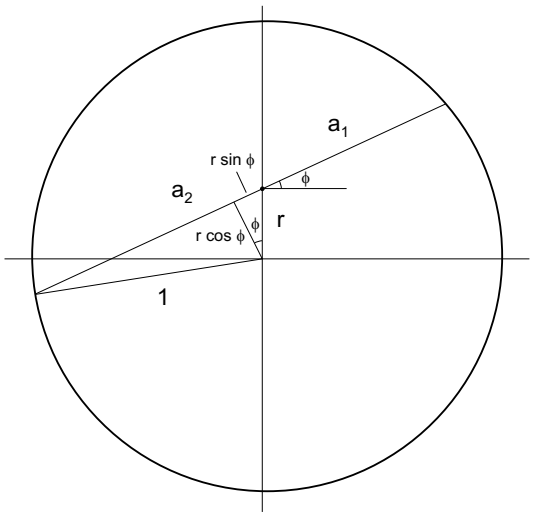

Figure 5: Derivation of a_1 and a_2 in a unit disk.

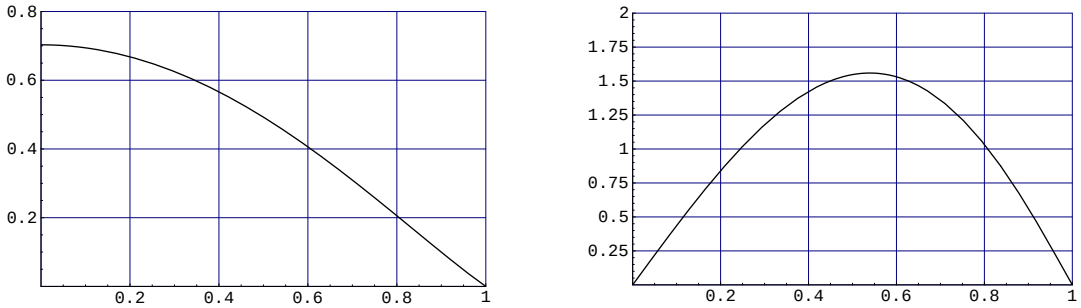

Figure 6: The pdf of the node location, $f(r)$, (left) and the pdf of the distance of a node from the origin, $f_R(r)$, (right) for a unit disk.

Thus we have $a_1 a_2 = 1 - r^2$ and $(a_1 + a_2) = 2\sqrt{1 - r^2 \cos^2 \phi}$, whence

$$h(r) = 2(1 - r^2) \int_0^{\pi} \sqrt{1 - r^2 \cos^2 \phi}\, d\phi. \tag{5}$$

This elliptic integral cannot be expressed in terms of elementary functions. However, one can evaluate the normalization constant in a closed form,

$$C = \int_{\mathcal{A}} h(\mathbf{r})\, d^2\mathbf{r} = 2\pi \int_0^1 r\, h(r)\, dr = \frac{128\,\pi}{45} = 8.936.$$

Thus, the pdf of the node location $\mathbf{R}$ is simply $f(r) = h(r)/C$. In Figure 6, $f(r)$ is depicted as a function of r along with the probability density function, $f_R(r) = 2\pi r\, h(r)/C$, of the random variable $R = |\mathbf{R}|$.

Then we have the average length of a leg from (1),

$$\overline{\ell} = \frac{C}{\pi^2} = \frac{128}{45\pi} \approx 0.905.$$

The result can also be derived using (4). In this case the area of the intersection $B(\mathbf{r})$ does not depend on the direction of the translation but is just a function of r, the length of the translation, $B(\mathbf{r}) = B(r)$, and equals twice the area of the segment of a unit disk as shown in Figure 7.

Thus we have

$$\overline{\ell} = \frac{2\pi}{A^2} \int_0^2 dr\; r^2 B(r),$$

where

$$B(r) = 2 \arccos\left(\frac{r}{2}\right) - r \sqrt{1 - \left(\frac{r}{2}\right)^2}.$$

The integral can again be evaluated explicitly and we obtain

$$\overline{\ell} = \frac{128}{45\pi} \approx 0.905,$$

in accordance with the previous result.

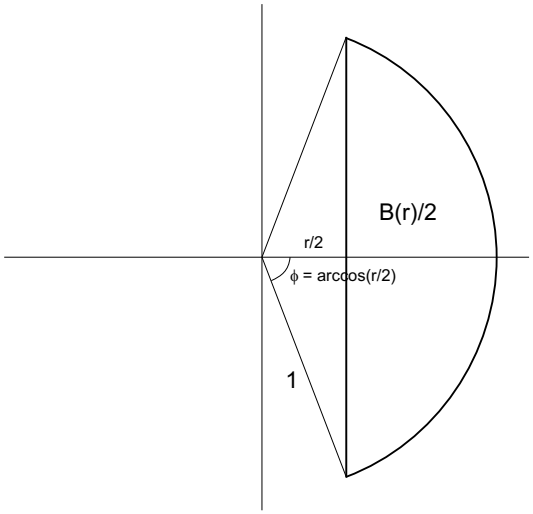

Figure 7: Illustration of the translation for unit disk.

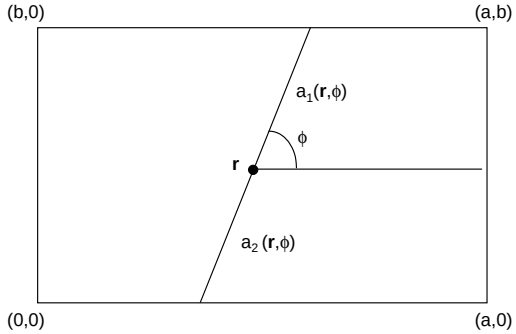

Figure 8: Illustration of the rectangle area.

3.3 Example: rectangular area

Consider a rectangular area with corner points at $(0,0)$, $(a,0)$, $(b,0)$ and (a,b). From Figure 8 it is easy to see that now we have for $\mathbf{r} = (x,y)$,

$$a_1(x,y,\phi) = \begin{cases} \frac{b-y}{\sin\phi}, & \arctan\frac{b-y}{a-x} \le \phi < \frac{\pi}{2} + \arctan\frac{x}{b-y}, \\ \frac{-x}{\cos\phi}, & \frac{\pi}{2} + \arctan\frac{x}{b-y} \le \phi < \pi + \arctan\frac{y}{x}, \\ \frac{-y}{\sin\phi}, & \pi + \arctan\frac{y}{x} \le \phi < \frac{3\pi}{2} + \arctan\frac{a-x}{y}, \\ \frac{a-x}{\cos\phi}, & 0 \le \phi < \arctan\frac{b-y}{a-x} \text{ or } \frac{3\pi}{2} + \arctan\frac{a-x}{y} \le \phi < 2\pi. \end{cases}$$

Note that in (1), as mentioned earlier, $a_2(\mathbf{r},\phi) = a_1(\mathbf{r},\phi+\pi)$.

To evaluate $\overline{\ell}$, which is needed in the normalization of (1), we use (4) for which we now have $B(r,\phi) = (a - r\cos\phi)^+(b - r\cos\phi)^+$. Due to symmetry it is sufficient to consider $\phi \in [0,\pi/2]$. We change the order of integration in (4) and eliminate the +-operator in $B(r,\phi)$ by introducing the function $g(\phi)$ which gives the proper integration range for r up

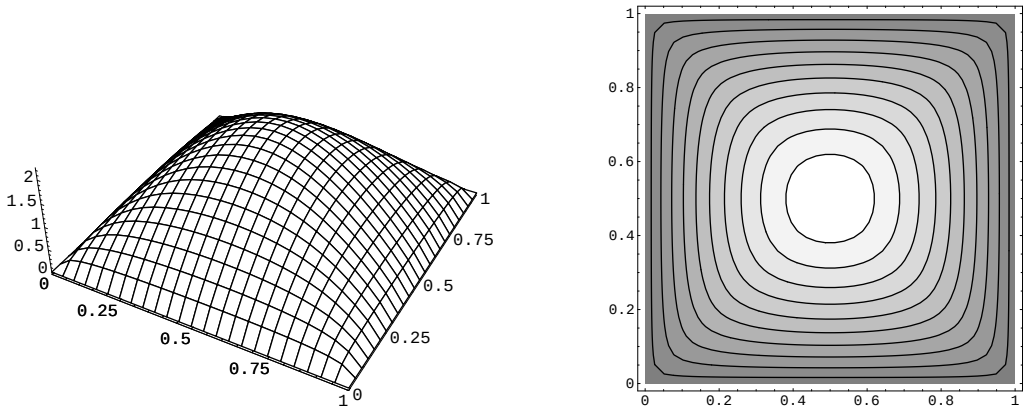

Figure 9: 3D plot of the pdf of the node location in a unit square (left) and its equivalue contours (right).

to which the areas of the rectangles still overlap in a given direction ϕ,

$$g(\phi) = \begin{cases} \frac{a}{\cos\phi}, & 0 \le \phi < \arctan\frac{b}{a}, \\ \frac{b}{\sin\phi}, & \arctan\frac{b}{a} \le \phi < \frac{\pi}{2}. \end{cases}$$

Hence, (4) can be expressed as

$$\begin{aligned} \overline{\ell} &= \frac{4}{a^2b^2}\int_0^{2\pi} d\phi \int_0^{g(\phi)} r^2(a - r\cos\phi)(b - r\cos\phi)dr \\ &= \frac{1}{a^2b^2}\int_0^{\pi/2} g(\phi)^3 \left(\frac{4}{3}ab - g(\phi)(b\cos\phi + a\sin\phi) + \frac{2}{5}g(\phi)^2\sin 2\phi\right) d\phi. \end{aligned}$$

The above integral can be easily evaluated numerically. For example for a unit square with $a = b = 1$ the above yields $\overline{\ell} = 0.521$ in accordance with results from [7]. As an example of the pdf in a rectangular area, Figure 9 shows the 3D plot (left figure) and the corresponding equivalue contours (right figure) for a unit square.

3.4 Example: polygon

Consider a general polygon. To numerically compute values of the pdf $f(\mathbf{r})$ we again need to first identify the form of $a_1(\mathbf{r}, \phi)$. In this case, for a given direction ϕ and location $\mathbf{r} = (x, y)$, the distance $a_1(\mathbf{r}, \phi)$ equals the distance to the straight line $c_1x + c_2y + c_3 = 0$ representing the edge of $\mathcal{A}$ in the direction ϕ, given by $a_1(x, y, \phi) = -(c_1x + c_2y + c_3)/(c_1\cos\phi + c_2\sin\phi)$. Integration over $[0, \pi]$ can then be carried out in parts between the angles at which $a_1(x, y, \phi)$ (and $a_1(x, y, \phi+\pi)$) crosses only one line segment. To evaluate $\overline{\ell}$ one can either use (3) or (4). Given that one already has an expression for $a_1(x, y, \phi)$ use of (3) is of course straightforward, but determining the function $B(r, \phi)$ and using (4) may be computationally more efficient.

As an example consider a pentagon with corner points $(3, 1), (1, 3), (-2, 2), (-1, -1)$ and $(3, -1)$. Integration of (2) over the area yields $C \approx 457.366$, and hence $\overline{\ell} = C/A^2 \approx 2.033$.

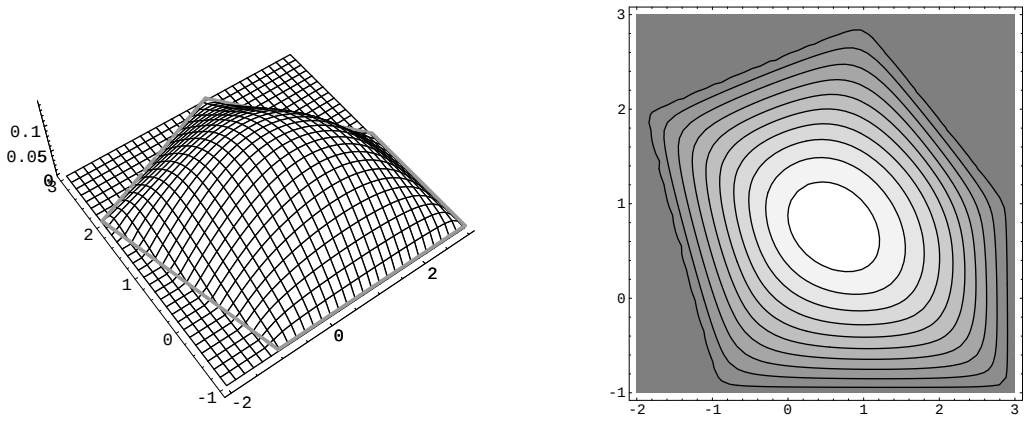

Figure 10: 3D plot of the pdf of node location in a pentagon area (left) and its equivalue contours (right).

Figure 10 shows the 3D plot of the pdf (left figure) and its equivalue contours (right figure).

3.5 Example: line segment

Finally, consider the simple case of a one-dimensional RWP on a line segment $(0, L)$, which represents a degenerate form of an ordinary two-dimensional RWP model in a rectangle with side lengths L and b in the limit $b \to 0$. Let $p(x)$ denote the probability that an arbitrary transition from x_i to x_{i+1} goes via some point x. It is easy to see that $p(x) = 2x(L-x)/L^2$ and hence $\mathrm{E}[\ell \cap dx] = p(x)\,dx$. Consequently,

$$f(x) = \frac{2x(L-x)}{\overline{\ell} L^2}. \tag{6}$$

The mean transition length $\overline{\ell}$ can be obtained by a straightforward integration or alternatively by normalizing (6), which yields

$$\overline{\ell} = L/3, \tag{7}$$

and thus

$$f(x) = \frac{6x(L-x)}{L^3}. \tag{8}$$

4 Analysis of RWPB

Let us consider the RWPB model introduced in Section 2.1, where the destination points are chosen uniformly on the border $\mathcal{B}$ of the area. In this case, it is also possible to perform

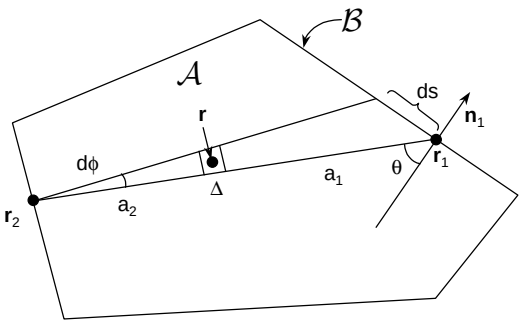

Figure 11: Notation for analysis of RWPB.

a similar general analysis as for the traditional RWP model. First the case of a general convex area is treated and then we consider a special case, namely the unit disk.

Consider first the case where the area $\mathcal{A}$ is convex and the curvature of the perimeter is positive everywhere. Hence, the perimeter does not contain any straight line segments and the probability of finding a node on the border is zero. To derive an expression for the node location distribution in this case, the initial steps in the analysis for the general convex area are basically the same as in the previous section for the standard RWP model, only the integrals are not over an area $\mathcal{A}$ but over a curve $\mathcal{B}$ with the length of the curve denoted by B. Now refer to Figure 11, where $\mathbf{r}_1$ and $\mathbf{r}_2$ are two waypoints on the border. In the figure $dA = a_2 \cdot d\phi \cdot \Delta$ and $\mathbf{n}_1$ denotes the unit normal vector at $\mathbf{r}_1$. To compute the conditional expectation $\mathrm{E}\left[\ell \cap dA \,|\, \mathbf{r}_2\right]$, it can be seen that the integral equals Δ times the length of the line segment ds along the edge. Using the notation of the figure we obtain

$$\mathrm{E}\left[\ell \cap dA \,|\, \mathbf{r}_2\right] = \frac{1}{B}\Delta ds = \frac{\Delta}{B}\frac{(a_1 + a_2) \cdot d\phi}{\cos\theta} = \frac{1}{B} dA \cdot \frac{a_1 + a_2}{a_2} \cdot \frac{1}{\cos\theta}.$$

Substituting this back in the original definitions gives

$$f(\mathbf{r}) = \frac{1}{\overline{\ell} B^2} \int_{\mathcal{B}} \frac{a_1 + a_2}{a_2 \cos\theta}\, ds, \tag{9}$$

where $a_1 = |\mathbf{r} - \mathbf{r}_1|$, $a_2 = |\mathbf{r}_2 - \mathbf{r}|$ and $\cos\theta = \mathbf{n}_1 \cdot (\mathbf{r}_1 - \mathbf{r}_2)/|\mathbf{r}_1 - \mathbf{r}_2|$.

Now let us return to the question of an area $\mathcal{A}$ the perimeter of which may contain straight line segments. Assume that there are k line segments on the border of $\mathcal{B}$ with lengths B_i, $i = 1, \ldots, k$, while the total length of the border is B. There is clearly a strictly positive probability that two consecutive waypoints reside on the same line segment and, consecutively, that the node is on the border, i.e., $\mathbf{R} \in \mathcal{B}$. Thus, the system can be seen to be in two alternating states: "border mode" and "interior mode". The border mode corresponds to legs along some straight line segment and the interior mode corresponds to legs passing through the area. In particular, let p_i denote the probability that an arbitrary leg occurs on line segment i,

$$p_i = \mathrm{P}\{\text{two consecutive waypoints on line segment } i\} = \left(\frac{B_i}{B}\right)^2,$$

and p_0 the probability that a transition belongs to interior mode, for which we have

$$p_0 = 1 - \sum_{i=1}^{k} p_i.$$

As the arriving point and the departing point on any line segment i are uniformly distributed, the two modes (interior/border) can be treated separately. Thus, point $\mathbf{R}$ has a one-dimensional pdf on each line segment on the border of $\mathcal{B}$, which are simply weighted versions of the one-dimensional RWP model pdf given by (8). Correspondingly, in the interior mode the probability density of the nodes obeys (9) with an appropriate weight.

The appropriate weights for interior mode and border modes are equal to the respective time proportions. Let π_0 denote the proportion of time the node spends in the interior mode and π_i, $i = 1, \ldots, k$, the proportion of time it spends on line segment i. For the π_i we have the obvious relation,

$$\pi_j = \frac{p_j \overline{\ell}_j}{\sum_{i=0}^{k} p_i \overline{\ell}_i}, \tag{10}$$

where $\overline{\ell}_i$ corresponds to the mean transition length on segment i. According to (7) the mean transition length on line segment i is $\overline{\ell}_i = B_i/3$, and thus

$$\pi_0 = \frac{p_0 \overline{\ell}_0}{p_0 \overline{\ell}_0 + \sum_{i=1}^{k} p_i B_i/3}. \tag{11}$$

In order to complete the analysis one still needs to determine the mean transition length in the interior mode, $\overline{\ell}_0$, which can be achieved by a straightforward integration or by normalizing (9).

In summary, the RWPB node distribution can be characterized as follows. With probability π_0 the point lies in the interior of $\mathcal{A}$ and its conditional two-dimensional density is given by (9). With probability π_i the point is on line segment i and its conditional one-dimensional density follows (8) with $L = B_i$.

Note that in fact one could also consider a modified process, where conditioned on that the current waypoint resides on some line segment, the next waypoint is be picked randomly from the (border) curve from which the current line segment has been removed. The interior point probability distribution of this process is directly given by (9) and the probability of finding the point on the border is zero.

4.1 Example: unit square

Consider next a unit square in which a point moves according to the RWPB model. Due to the symmetry we can concentrate on x-axis first. In this case the mean transition length in

interior mode can be obtained by a straightforward integration,

$$\begin{aligned}\overline{\ell}_0 &= \frac{2}{3}\int_0^1\int_0^1 \sqrt{x^2+y^2}\,dx\,dy + \frac{1}{3}\int_0^1\int_0^1 \sqrt{(x-y)^2+1}\,dx\,dy \\ &= \frac{1}{9}\left(2+\sqrt{2}+5\ln(1+\sqrt{2})\right) \approx 0.869.\end{aligned}$$

Thus, the proportion of time the point spends in the interior mode is

$$\pi_0 = \frac{2+\sqrt{2}+5\ln(1+\sqrt{2})}{3+\sqrt{2}+5\ln(1+\sqrt{2})} \approx 0.887,$$

and similarly, the proportion of time on each border line segment is,

$$\pi_i = \frac{1/4}{3+\sqrt{2}+5\ln(1+\sqrt{2})} \approx 0.0283, \qquad i = 1,\ldots,4.$$

At this point one can immediately write down the one-dimensional pdf on each border line segment,

$$f_i(x) = \pi_i \cdot 6x(1-x) = \frac{3x(1-x)}{6+2\sqrt{2}+10\ln(1+\sqrt{2})}, \qquad i = 1,\ldots,4.$$

The two-dimensional pdf corresponding to interior points can be obtained by evaluating (9) and multiplying it by π_0.

4.2 Example: unit circle

Above we have derived a general result (9) for the distribution of a point inside a given area when the waypoints are evenly distributed on the perimeter. The expression is somewhat complicated and difficult to apply for specific geometries. Here we derive the result in a more direct way for the unit circle. In fact, we can generalize the model a bit. Instead of assuming that the next waypoint is chosen uniformly on the perimeter, we assume that the direction of the leg from the present waypoint to the next, defined by the angle ϕ between the radius to the current waypoint and the leg (see Figure 12), also called the "bouncing angle", is randomly drawn from a distribution with a given pdf $f_\phi(\phi)$. It is easy to see that the uniform distribution $\phi \sim U(-\pi/2, \pi/2)$ corresponds to a uniform distribution of the waypoint on the perimeter.

We wish to calculate the radial distribution, $F_R(r)$, of distance $R = |\mathbf{R}|$,

$$F_R(r) = \mathrm{P}\{|\mathbf{R}| \le r\}.$$

To this end, let $\ell(\phi)$ be the length of a random leg and $d(r,\phi)$ the length of the segment of $\ell(\phi)$ inside the circle of radius r, see Figure 12. Both $\ell(\phi)$ and $d(r,\phi)$ are functions of the random variable ϕ. The required probability $F_R(r)$ is now given by $\overline{d}(r)/\overline{\ell}$, where $\overline{d}(r) = \mathrm{E}[d(r,\phi)]$ and $\overline{\ell} = \mathrm{E}[\ell(\phi)]$,

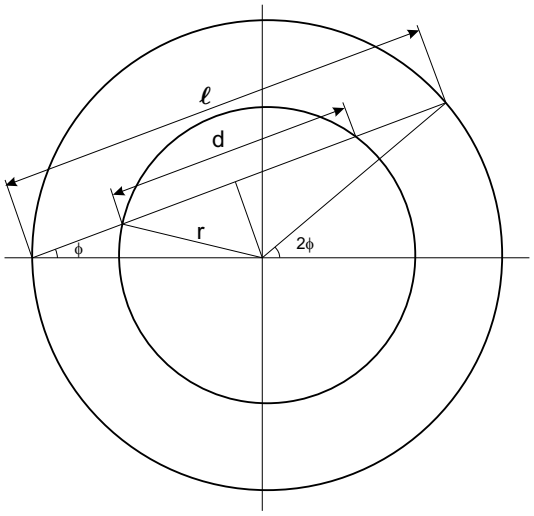

Figure 12: Notation for analysis of RWPB in a unit circle.

For a given ϕ we have from Figure 12,

$$\begin{cases} d(r,\phi) &= 2\sqrt{r^2-\sin^2\phi}, \\ \ell(\phi) &= 2\sqrt{1-\sin^2\phi} \quad = \quad 2\cos\phi. \end{cases}$$

Denote by ϕ_0 the angle at which $d(r,\phi)=0$,

$$\phi_0(r) = \arcsin r.$$

With the pdf $f_\phi(\phi)$ we then have the expected values,

$$\begin{cases} \overline{d}(r) &= 2\displaystyle\int_0^{\phi_0} d(r,\phi) f_\phi(\phi)\, d\phi, \\ \overline{\ell} &= 2\displaystyle\int_0^{\pi/2} \ell(\phi) f_\phi(\phi)\, d\phi, \end{cases}$$

which lead to the result

$$F_R(r) = \frac{\overline{d}(r)}{\overline{\ell}} = \frac{\displaystyle\int_0^{\phi_0} \sqrt{r^2-\sin^2\phi}\, f_\phi(\phi)\, d\phi}{\displaystyle\int_0^{\pi/2} \sqrt{1-\sin^2\phi}\, f_\phi(\phi)\, d\phi}.$$

For the uniform distribution, $f_\phi(\phi) = 1/\pi$ for $\phi \in (-\pi/2, \pi/2)$ and 0 otherwise, the expressions simplify:

$$\overline{\ell} = \frac{2}{\pi}\int_0^{\pi/2} 2\,\cos\phi\, d\phi = \frac{4}{\pi}$$

and

$$F_R(r) = \int_0^{\phi_0} \sqrt{r^2-\sin^2\phi}\, d\phi. \tag{12}$$

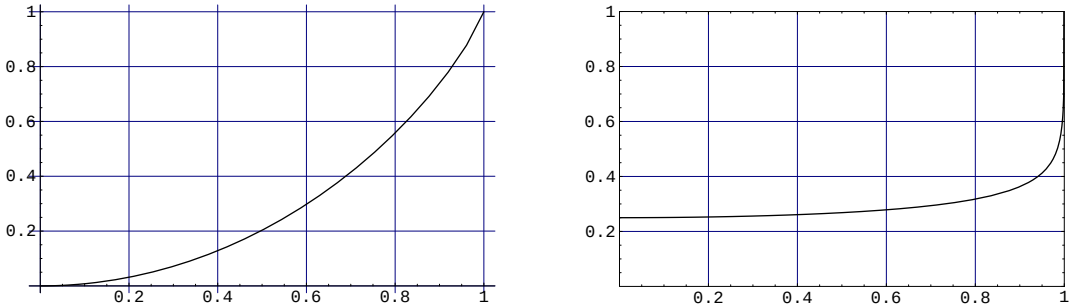

Figure 13: The cdf $F_R(r)$ of the distance of the node from the origin (left) and the pdf $f(\mathbf{r}) = f(|\mathbf{r}|)$ of the node location (right) for the RWPB model in a unit disk.

RWPB with uniform angle distribution in a unit disk is illustrated in Figure 13, where the left graph shows the cumulative distribution function (cdf) $F_R(r)$ of the distance from the center and the right graph shows the probability density function of the point location at distance r in any direction, $f(\mathbf{r}) = f(r) = F_R'(r)/2\pi r$. From the right figure it can be seen that the density increases towards the perimeter. Recall that for the ordinary RWP model the density decreases to zero towards the border (cf. Figure 6). This suggests that it should be possible to devise an RWP model with a non-uniform distribution of waypoints $\mathbf{X}$ which leads to a uniform distribution of the node location $\mathbf{R}$.

5 Efficient simulation of the RWP model

As before we denote by $\mathbf{R}$ the random variable representing the position of a node moving according to the RWP model without think times. Consider estimating by simulation the expectation

$$H = \mathrm{E}[f(\mathbf{R})].$$

An estimator with N samples is given by the sample mean

$$\hat{H} = \frac{1}{N} \sum_{n=1}^{N} f(\mathbf{R}_n), \tag{13}$$

where $\mathbf{R}_n$ denotes the nth sample of $\mathbf{R}$.

To generate the $\mathbf{R}_n$, there are basically two different approaches: process simulation and static Monte Carlo simulation. In process simulation consecutive samples are typically positively correlated, whereas in static Monte Carlo the samples are independent. From the simulation point of view, independent samples are more efficient as the variance of (13) is smaller. Note that if the simulation scenario requires use of several nodes moving according to the RWP model, the location of each node is independent of the others.

In the following we utilize the analytical results derived earlier and give several methods to efficiently generate samples of $\mathbf{R}$ in a general convex area $\mathcal{A}$. For the case of a unit disk, the

distribution is simply a function of the distance from the center and an explicit solution can be given for it. Hence, the standard inverse transformation method (see, e.g., [12]) could be directly applied to that. For more general geometries the use of the inverse transformation method is more difficult as it requires the inversion of the cumulative distribution functions of, for instance, the x-component of the location and then the y-component conditioned on x. However, we can still take advantage of our analytical results and devise efficient sample generation algorithms.

5.1 Process simulation with exponential sampling

Process simulation is the most straightforward method to simulate the RWP process. Briefly, a separate process is needed to draw samples of the waypoints $\mathbf{X}$. To draw a sample of $\mathbf{R}$, a sampling process that samples the location of the RWP node with exponentially distributed time intervals is needed (i.e., the PASTA property is utilized). Note that, the location of a point, $\mathbf{R}$, becomes independent of the earlier locations after two waypoints.

The idea is to generate the waypoints and then draw samples along the line segments between the waypoints with exponentially distributed intervals with mean d. Sampling with a very small d is not desirable as the consecutive points are then heavily positively correlated, but making the interval d too long results in that we often do not get any samples between two waypoints. A reasonable choice for the interval is to set $d \approx \overline{\ell}$. The following pseudo-code illustrates the simulation procedure:

1. Initialize:
   (a) Draw locations of two waypoints $\mathbf{X}_1 \sim \mathrm{U}(\mathcal{A})$ and $\mathbf{X}_2 \sim \mathrm{U}(\mathcal{A})$.
   (b) Draw $W \sim \mathrm{Exp}(1/d)$.
2. While more samples needed,
   (a) While $W < |\mathbf{X}_2 - \mathbf{X}_1|$,
   New sample $\mathbf{R} = \mathbf{X}_1 + W \cdot (\mathbf{X}_2 - \mathbf{X}_1)/|\mathbf{X}_2 - \mathbf{X}_1|$,
   $\mathbf{X}_1 \leftarrow \mathbf{R}$,
   Draw $W \sim \mathrm{Exp}(1/d)$,
   End while.
   (b) $\mathbf{X}_1 \leftarrow \mathbf{X}_2$, draw $\mathbf{X}_2 \sim \mathrm{U}(\mathcal{A})$,
   End while.

Alternatively at point 2.b above we may redraw both waypoints in order to get less correlated samples, i.e.,

b) Draw $\mathbf{X}_1 \sim \mathrm{U}(\mathcal{A})$ and $\mathbf{X}_2 \sim \mathrm{U}(\mathcal{A})$.

Note that in step 2.a, a set of (zero or more) correlated samples is produced. If the latter option for 2.b is adopted, the sets are independent.

5.2 Static Monte Carlo simulation with weighted samples

The following method produces always i.i.d. samples of $\mathbf{R}$ (hence the name static Monte Carlo). In this method two waypoints are generated and the sample point is randomly chosen from the line segment between these points. The idea is to utilize the fact that conditioned on the location of the two waypoints $(\mathbf{X}_1, \mathbf{X}_2)$ of a leg, the distribution of the location of $\mathbf{R}$ is uniformly distributed between $(\mathbf{X}_1, \mathbf{X}_2)$. The probability density that the point is on the considered line segment depends on the time spent on the leg. This can be taken into account by giving each generated point a weight that is proportional to the length of the line segment. The following pseudo code illustrates the method to generate a sample of the point $\tilde{\mathbf{R}}$ and its weight ℓ:

1. Draw two waypoints $\mathbf{X}_1 \sim \mathrm{U}(\mathcal{A})$ and $\mathbf{X}_2 \sim \mathrm{U}(\mathcal{A})$ and $U \sim \mathrm{U}[0,1]$.
2. Set $\tilde{\mathbf{R}} = U\mathbf{X}_1 + (1-U)\mathbf{X}_2$.
3. Set $\ell = |\mathbf{X}_2 - \mathbf{X}_1|$.

Using the above the estimator (13) changes to

$$\hat{H} = \frac{1}{\overline{\ell} \cdot N} \sum_{n=1}^{N} f(\tilde{\mathbf{R}}_n)\, \ell_n, \quad \text{with } \overline{\ell} = \frac{1}{N} \sum_{n=1}^{N} \ell_n.$$

Using the same data to estimate both H and ℓ obviously introduces bias in the estimator, which, however, should be negligible for realistic sample sizes. The impact of bias is investigated later in the numerical examples.

In [9] a similar process was used. There, instead of weights, a part of the generated points was rejected with a probability $p = \ell/D$, where D denotes the maximum diameter of the considered area $\mathcal{A}$. As seen from above, the simulation can be made more efficient by not rejecting samples, as long as the samples are weighted properly.

5.3 Rejection method

It is also possible to utilize the standard rejection method (see, e.g., [12]) to draw i.i.d. samples of $\mathbf{R}$. The most direct application of the method consists of finding a function $q(\mathbf{r})$ such that $q(\mathbf{r}) \geq f(\mathbf{r})$. However, it is possible to go even further in the method and to avoid the integration over $[0, \pi]$ required by (1). Basically, the idea is to generate a random point in $\mathcal{A}$ and a random angle and to accept the point with a probability proportional to the integrand in (1). A pseudo code for the sample generation is the following:

1. Draw a sample of $\mathbf{R} \sim \mathrm{U}(\mathcal{A})$ and $\phi \sim U[0, \pi]$.

2. Accept $\mathbf{R}$ with probability p,

$$p = \frac{a_1(\mathbf{R}, \phi) a_2(\mathbf{R}, \phi)(a_1(\mathbf{R}, \phi) + a_2(\mathbf{R}, \phi))}{m},$$

where $m = \max_{\mathbf{r} \in \mathcal{A},\, \phi \in [0,\pi]} \{\, a_1(\mathbf{r}, \phi) a_2(\mathbf{r}, \phi)(a_1(\mathbf{r}, \phi) + a_2(\mathbf{r}, \phi)) \,\}$.

For the above rejection method it is also possible to compute the theoretical acceptance ratio of the samples. Given the point $\mathbf{R}$ and the angle ϕ, the acceptance probability is p. The overall acceptance probability $\overline{p}$ is then obtained by integrating p first over the distribution of $\phi \sim U[0, \pi]$ and then over the distribution of the points $\mathbf{R}$. For simplicity we omit the arguments from the functions a_1 and a_2. Thus, using (2) and (3) we get

$$\overline{p} = \frac{1}{\pi \cdot mA} \int_{\mathcal{A}} \int_0^{\pi} a_1 a_2 (a_1 + a_2) d\phi d^2\mathbf{r} = \frac{\overline{\ell} \cdot A}{\pi \cdot m}.$$

For the unit disk with $m = 2$ and $\ell = 128/(45\pi)$ this gives $\overline{p} = 64/(45\pi) \approx 0.453$. For the unit square with $m = \sqrt{2}/2$ and $\overline{\ell} \approx 0.521$ we obtain $\overline{p} \approx 0.235$.

5.4 Numerical examples

In order to compare the performance of the methods described above we generated points from the RWP model in a unit circle and estimated $H = \mathrm{E}[|\mathbf{R}|]$. New samples were generated until the relative error of the estimate, defined as $\sqrt{\mathrm{Var}[\hat{H}_N]}/\hat{H}_N$ with $\hat{H}_N$ denoting the estimate after N samples have been drawn, was below a predefined value (target value of 0.001 was used in the examples). The required computational effort was studied by measuring both the simulation time and the number of the sample points needed. The methods were implemented in Mathematica 5.0 and executed on a standard PC with an AMD Athlon 1.4 GHz processor. The results are summarized in Table 1. In our exponential sampling implementation we have used the option of redrawing both waypoints after reaching the end of a leg and the sampling interval was chosen such that $d = \overline{\ell} = 0.905$.

As can be expected, the weighted samples method gives samples with highest variability (due to the weighting), and the most efficient samples are obtained by using the rejection method. However, in the rejection method the table shows the number of accepted samples and, as discussed earlier, the acceptance ratio for the method in a unit disk equals roughly 0.5 and thus the total number of samples (accepted and rejected) is actually twice as high (the time reported in Table 1 includes the total time to generate both the accepted and rejected samples). The exponential sampling method is somewhat worse than the rejection method in variance performance due to the positive correlations between the samples. The execution times given in the table should be taken only as indicative and are subject to implementation related differences. Additionally, for the rejection method the form of the

Table 1: Required work for different simulation methods.

simulation method	time (s)	samples
exponential sampling	91	271 400
weighted sampling	92	408 700
rejection method	57	183 500

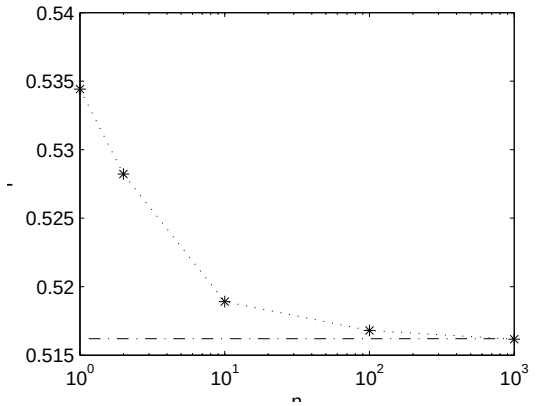

Figure 14: Simulation of the RWP model with weighted samples method. The bias of the estimator diminishes quickly as the number of samples increases.

acceptance criterion function is relatively easy to compute in the case of the unit disk, and that may have given the method an advantage that does not apply for all geometries.

As discussed earlier in Section 5.2, the estimation of $\overline{\ell}$ at the same time as the interesting quantity H introduces bias in the estimate. Figure 14 illustrates how the bias quickly diminishes as the number of RWP points generated increases. In the figure the straight dashed line indicates the unbiased target value. Each simulated point represent a mean of 1000 replicas of the estimator of a given sample size. From the figure it can be seen that with a sample size of 100 points or higher the bias in the estimate due to estimating $\overline{\ell}$ from the same samples becomes negligible.

6 Conclusions

One of the most widely used mobility models is the RWP model. We have analyzed two intrinsic stochastic properties of the model, namely the spatial distribution of a node moving according to the RWP model and the mean length of a leg. The main result of our paper is the general expression giving the node distribution up to a normalization constant. The expression consists of a one-dimensional integral, which is easy to evaluate numerically for any given geometry. The mean length of a leg can be expressed in two alternative ways, either by relating it to the normalization constant of the node distribution or directly by start-

ing from the definition of the mean length. Both expressions are basically two-dimensional integrals. The results have been illustrated for several geometries: unit circle, rectangle, pentagon and line. In general the shape of the node distribution for any geometry is such that the probability mass is concentrated in the center of the area, where the equivalue contours are circular/elliptical, and the density decreases roughly linearly towards the borders with the equivalue contours gradually transforming to curves resembling the geometry of the considered area.

We have additionally analyzed the RWPB model, where the waypoints are chosen always on the border of the area. If the border contains straight line segments, the distribution of the location of the node is composed of two components corresponding to the border mode and the interior mode. We have given general expressions for both components of the node distribution. Explicit result for the unit circle, having only the interior component, has been derived. In general, the node distribution in the RWPB model differs from the RWP model by concentrating the probability mass near the border of the area and, indeed, yielding a non-zero probability mass on the border if it contains straight line segments.

Finally, the problem of efficient sample generation of points from the node distribution for simulation purposes has been studied. Three different algorithms have been proposed and their performance has been compared through numerical examples. The weighted samples method gives less efficient samples (more variance resulting from the weighting) than the rejection method, but the rejection method requires calculating the functions $a_1(\mathbf{r}, \phi)$ and $a_2(\mathbf{r}, \phi)$.

Future research includes generalization of the results to N-dimensional space. Additionally, in the simulation methods, the rejection method can be greatly improved by defining more sophisticated majorizing functions to increase the acceptance ratio. A further challenge is to solve the inverse problem, i.e., to find for the waypoint $\mathbf{X}$ such a distribution that the resulting node distribution is uniform $\mathbf{R} \sim \mathrm{U}(\mathcal{A})$. As indicated at the end of Section 4.2 this is probably a well-posed problem admitting a solution.

Acknowledgment

This work has been partially funded by the Finnish Defence Forces Technical Research Center and by the Academy of Finland (grants n:o 202204 and 74524).

References

[1] M. Grossglauser and D. N. C. Tse, "Mobility increases the capacity of ad hoc wireless networks," *IEEE/ACM Transactions on Networking*, vol. 10, no. 4, August 2002.

[2] P. Gupta and P. R. Kumar, "The capacity of wireless networks," *IEEE Transactions on Information Theory*, vol. 46, no. 2, March 2000.

[3] O. Dousse, P. Thiran, and M. Hasler, "Connectivity in ad-hoc and hybrid networks," in *Proceedings of IEEE INFOCOM*, New York, June 2002.

[4] H. Koskinen, "A simulation-based method for predicting connectivity in ad hoc networks," in *Proceedings of INOC 2003*, Evry/Paris, France, October 2003.

[5] D. B. Johnson and D. A. Maltz, *Dynamic source routing in ad hoc wireless networks*, T. Imilinski and H. Korth, Eds. Kluwer Academic Publishers, 1996.

[6] C. Bettstetter and C. Wagner, "The spatial node distribution of the random waypoint mobility model," in *Proceedings of German Workshop on Mobile Ad Hoc networks (WMAN)*, Ulm, Germany, March 2002.

[7] C. Bettstetter, G. Resta, and P. Santi, "The node distribution of the random waypoint mobility model for wireless ad hoc networks," *IEEE Transactions on Mobile Computing*, vol. 2, no. 1, pp. 25–39, 2003.

[8] C. Bettstetter, H. Hartenstein, and X. Pérez-Costa, "Stochastic properties of the random waypoint mobility model," *to appear in ACM/Kluwer Wireless Networks: Special Issue on Modeling and Analysis of Mobile Networks*, 2003. [Online]. Available: http://www.lkn.ei.tum.de/~chris/#Publications

[9] W. Navidi and T. Camp, "Stationary distributions for the random waypoint mobility model," *to appear in IEEE Transactions on Mobile Computing*, 2003, technical Report MCS-03-04, The Colorado School of Mines.

[10] J. Broch, D. A. Maltz, D. B. Johnson, Y. C. Hu, and J. Jetcheva, "A performance comparison of multihop wireless ad hoc network routing protocols," in *Proceedings of ACM International Conference on Mobile Computing and Networks (MOBICOM)*, Dallas, TX, USA, October 1998.

[11] J. Yoon, M. Liu, and B. Noble, "Random waypoint considered harmful," in *Proceedings of IEEE INFOCOM*, San Fransisco, California, USA, April 2003, pp. 1312–1321.

[12] A. M. Law and W. D. Kelton, *Simulation modeling and analysis*, 3rd ed. New York, USA: McGraw-Hill, 2000.